Physics of Nickel Clusters: Energetics and Equilibrium Geometries

Saroj K. Nayak, S. N. Khanna, B. K. Rao, and P. Jena*

Physics Department, Virginia Commonwealth University, Richmond, Virginia 23284

Received: September 5, 1996; In Final Form: October 22, 1996[⊗]

The equilibrium geometries and the binding energies of Ni_n clusters ($n \leq 23$) have been calculated by using an empirical many-body potential and molecular dynamics (MD) simulation. For small clusters, the potential is found to reproduce the geometries based on first-principles density functional calculations. It is shown that the clusters do not mimic the bulk structure and undergo significant geometrical changes with size. The binding energy per atom, on the other hand, increases monotonically with size. The evolution of the geometries is found to be correlated with the underlying changes in the nature of bonding. An analysis of the fragmentation channels based on the ground state energies shows the loss of the Ni dimer to be the most energetically favorable channel. The calculated geometries are compared with those derived from recent experiments on N_2 adsorption on Ni_n clusters.

I. Introduction

The field of atomic clusters has received widespread attention since the geometries and electronic, magnetic, and chemical properties of clusters are found to be different from the bulk.[1−3] The properties often evolve non-monotonically with size, and the possibilities of making new materials by assembling clusters with tailored properties are being envisioned.[4] The novelty in clusters is largely due to the fact that their geometrical structures are unique and are governed by the local chemical bonding instead of the long-range order as in the bulk. An understanding of the evolution of the equilibrium geometries and its relationship to the underlying electronic structure are, therefore, of central importance. Despite vast progress in our understanding of the physics of clusters in the last decade, certain basic issues remain mostly unsolved. For example, there is no experimental technique that can directly yield the geometries of small clusters. Structures of atomic clusters consisting of a few hundred atoms or less are too small to be probed by diffraction techniques and too large to be probed by spectroscopic techniques. However, it is in this size range that clusters exhibit their unique size-specific properties. The study of atomic structures of clusters has, therefore, been left to indirect experimental methods and/or theoretical calculations. For simple metals, for instance, the electron spin resonance or negative ion photoelectron spectroscopy combined with ab initio calculations[5−16] is being used to derive information on geometries. For transition metals, the situation is unclear. These metals are characterized by unfilled valence d-orbitals, which complicate the description because of their localization and high density of states. On the experimental side, efforts are being made to probe the structure via chemical methods.[17] Here, one reacts the metal clusters with a weakly interacting gas such as N_2 and studies the number of adsorbed molecules as a function of temperature and pressure. Assuming that different surface sites have different affinity for binding N_2's, the number of adsorbed molecules can give an indication of the number of inequivalent metal sites, from which one can derive a geometrical structure. This approach has recently been used by Riley and co-workers[17] to propose geometries of Ni_n clusters, $n < 28$.

The d-states offer a particular challenge for the theory. The number of states and their localized character require extensive computational resources. There have been only limited ab initio studies with differing level of complexity. Earlier attempts made use of the Hatree−Fock[6,7,12] or the density functional method[5,9] to study transition metal clusters confined to selected geometries. While providing detailed electronic structure, these methods did not carry out global geometry optimization, which is germane to small clusters. Attempts were also made to carry out studies ignoring the d-states altogether.[10] It is only very recently that realistic calculations with optimized geometries were attempted.[13−15] Unfortunately, these are computer intensive and have been confined to clusters having less than 10 atoms. In addition, the results depend on the approximations made in the ab initio calculations. For example, the equilibrium geometries and energies of Fe_n clusters ($n < 7$) have been computed using Car-Parrinello molecular dynamics simulations[14] and molecular orbital theory.[13] In the former method, the electron−ion interaction is treated by a pseudopotential and electron orbitals are expanded in a plane wave basis. In the molecular orbital theory, the electron orbitals are expressed by a Gaussian basis. Both the schemes employ the spin density functional method. Although the geometries obtained by these authors agree with each other, the energetics do not. The binding energy of the ground state of Fe_2 obtained by Ballone and Jones[14] is 3.81 eV, while that obtained by Castro and Salahub is 2.08 eV. The corresponding experimental value is 1.14 eV. Similarly for Fe_3 the binding energy calculated from the ab initio MD method is 3.04 eV, which is considerably larger than that predicted by molecular orbital theory, namely, 1.41 eV. This discrepancy persists for larger clusters too. Although, more accurate ab initio MD could be carried out, such calculations are computationally too expensive and hence are only restricted for studying small clusters ($n < 7$). Since most of the experiments are carried out on clusters containing up to several dozen atoms, it is clear that there is a need for methods capable of providing information at these sizes.

A way out of these limitations is to use molecular dynamics simulation and model many-body potentials.[18,19] There are a number of approaches that are currently being pursued. One of these methods is based on the embedded atom model.[20,21] Here, the many-body potential is expressed as a sum of a pairwise term and a term that takes into account many-body effects. The many-body effects appear through the inhomogeneous electron charge density obtained by superposing atomic electron densities. The many-body component of the potential is a functional of the electron density and is usually calculated

[⊗] Abstract published in *Advance ACS Abstracts,* January 15, 1997.

S1089-5639(96)02720-X CCC: $14.00

in a local approximation. The parameters appearing in this formulation are usually fitted to bulk cohesive energy and dimer potential energy curves. This approach has been used by Stave and De Pristo[21] to calculate the structure of Ni_n clusters up to 23 atoms. A different approach is to use analytic two- and three-body potentials.[22] The parameters entering the potential can be determined either by fitting to ab initio Born−Oppenheimer surfaces on small clusters or to the selected bulk properties. While the former approach provides a way of extending ab initio calculations to larger sizes, the latter can give an idea about the applicability of bulk interatomic interactions at smaller sizes. The analytical potentials are particularly attractive for studying cluster dynamics at elevated temperatures. An attempt along these lines was recently made by Jellinek *et al.*[18] They used a many-body form proposed by Gupta,[23] which is a generic form applicable to all transition metals. The structures based on this potential were at variance with those based on effective medium theory.[21] It is not clear whether this discrepancy is due to differences in the treatment of the many-body potential or due to the fact that the parameters of the Gupta potential are not suitable for small clusters.

In this paper we provide the results of a molecular dynamics study of Ni_n clusters (up to 23 atoms) using the potential developed by Finnis and Sinclair.[24] These potentials are based on tight binding total energy calculations and contain many-body terms. They are distinct from the conventional two-body potentials, and the reader is referred to a recent paper by Sutton *et al.*[25] for details. We have developed a new numerically efficient scheme for obtaining ground state geometries. The scheme is a variant of the conventional simulated annealing[26] and allows an efficient approach to the ground state via *configurational energy*. We first demonstrate the validity of the potential by comparing the calculated geometries of small Ni_n ($n \leq 6$) clusters with those based on ab initio density functional studies. We then use it to study the geometries and energetics of larger clusters ($23 \geq n > 6$). Our results agree with those based on effective medium theory and experiment. It is shown that while the binding energies increase monotonically with size, the geometries can change substantially even with the addition of a single atom. The change in geometry is linked to the underlying electronic structure of clusters. For many sizes we find energetically close isomers with different symmetries. The implication of the existence of isomers on observed properties will be discussed. The energies are used to examine the fragmentation channels.[27] For all sizes the energetically most preferred channel is the loss of Ni_2.

In section 2, we describe the potential and the method used to optimize the geometries. The results are discussed in section 3 and summarized in section 4.

II. Interatomic Potential and Computational Techniques

Molecular dynamics is a powerful method to probe the equilibrium geometries, stability, fragmentation channels, and melting of atomic clusters. The key requirement in this procedure is the interatomic potential. While the quantum molecular dynamics method advanced by Car and Parrinello[28] eliminates the need for interatomic potentials, its applicability to transition metal systems has met with considerable difficulty, as outlined in the previous section. The choices of interatomic potentials for the transition metal series are still limited to empirical forms. Here the parameters are obtained by fitting the data to experiment in bulk systems such as cohesive energy, elastic constants, and lattice structure. One does not know a priori if such potentials are useful for studying the dynamics of clusters. It is, therefore, important that structures and energetics calculated using empirical interatomic potentials be compared with those obtained from first principles. This is the approach we have taken in this paper. The interaction between the atoms in a Ni cluster is taken from the work of Finnis−Sinclair[24] and Sutton and Chen.[29] The potential has the form

$$V = \epsilon \sum_i \left[\frac{1}{2} \sum_{j \neq i} \left(\frac{a}{r_{ij}} \right)^n - c\rho_i^{1/2} \right] \tag{2.1}$$

where

$$\rho_i = \sum_{j \neq i} \left(\frac{a}{r_{ij}} \right)^m \tag{2.2}$$

r_{ij} is the distance between the atoms i and j, a is the lattice constant, c is a dimensionless parameter, ϵ is the parameter with dimension of energy, and m and n are integers. The parameters in the above equation have the following values for Ni: $a = 3.52$ Å, $c = 39.432$, $\epsilon = 1.5707 \times 10^{-2}$ eV, $m = 6$, and $n = 9$.[29] The square root term in the attractive part of the potential accounts for many-body interaction. This potential has been shown to reproduce bulk and surface properties (e.g. relaxation of top layers) of transition metals with sufficient accuracy. For example, the calculated inward relaxation of top layers for 100, 110, and 111 faces are 2.9, 7.9, and 2.1,[30] in excellent agreement with experimental values of 3.2,[31] 8.6,[32] and 1.3,[33] respectively. Experimentally it is difficult to obtain the surface energy of each individual face. However, the surface energies obtained using the above potential are in close agreement with those obtained using embedded atom potentials.[34] Energetics of clusters with complete geometric shells (confined to icosahedric structures) in the size range 13−309 have also been obtained using the above form for metal clusters.[19]

We use constant energy molecular dynamics (MD) simulations[35] for determining structure and energetics of Ni_n, $n \leq 23$. The velocity Verlet algorithm[35] is used to integrate the classical equations of motions with a time step of 5×10^{-15} s. The total linear and angular momentum is kept zero,[36] and the energy is conserved to within 0.01%. Locating the global minimum structure is a tricky matter, particularly when the ground state is plagued by energetically close isomers. In these cases the conventional steepest descent method[37] is often unable to locate the absolute global minimum structure. The usual approach is then to use a simulated annealing,[26] where one heats the cluster to a very high temperature and gradually lowers the temperature, allowing it to nearly stabilize to equilibrium configuration at each step of the descent. The functional controlling the descent is the total energy.[28] We propose a different approach. Starting at a high temperature, the cluster is slightly cooled[38] and the change in *configurational energy* (not the total energy) is examined. The new configuration thus obtained is accepted if the difference in *configurational energy*, ΔE, between the state before and after cooling the system is negative. If $\Delta E \geq 0$, then the state is accepted with a probability given by $\exp(-\Delta E/k_b T)$: for $T \rightarrow 0$ the ground state is obtained. (It is easy to convince oneself that decreasing the kinetic energy always lowers the total energy but not necessarily the configurational energy: by selecting the path that lowers configurational energy, one arrives at the equilibrium configuration and avoids trapping the system in local minima.) This method is much faster than the usual simulated annealing approach using Metropolis sampling.[26,39] This happens because the moves in the present MD are usually biased in the direction of intermolecular forces whereas in Metropolis sampling one samples moves parallel or antiparallel to the forces with equal probability. Figure 1 shows

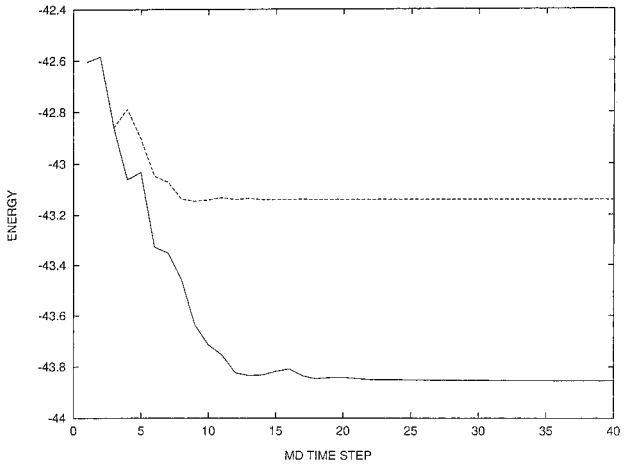

Figure 1. Plot of configurational energy of the Ni_{13} cluster versus MD time steps. Dashed line corresponds to the conventional simulated annealing method where the total energy is considered to be the functional in determining the equilibrium geometry, and solid line corresponds to the new method where the functional is the configurational energy. The cooling rates for both methods are the same.

a typical plot of configurational energy of a Ni_{13} cluster versus MD time steps. One can easily see that using the present method, the ground state energy is approached by an order of magnitude faster compared to the usual simulated annealing method, where the total energy is a functional.[28]

The most important consideration for interpreting the results in the following is to assess the validity of the interatomic potential in eq 2.1 in predicting the properties of Ni clusters. Note that this potential does not have any explicit spin-dependent term, and one, therefore, wonders if this could adversely affect the properties of Ni clusters, which are expected to be magnetic. To address this issue, it is important to realize that the parameters of eq 2.1 are obtained by fitting to bulk and surface properties of Ni in the ferromagnetic state. The magnetic moment at the surface is different than in the bulk, and this change occurs primarily due to change in coordination. Fitting the potential to both bulk and surface therefore implicitly incorporates the change in magnetic state via change in coordination in the total energy calculation. In the present molecular dynamics simulation we are interested in the atomic structure (i.e. equilibrium geometries) of Ni clusters. Since most of these atoms are surface atoms and the potential does reproduce surface reconstruction quite well, we do not expect the absence of a spin-dependent term in eq 2.1 to adversely affect the reliability of the computed equilibrium geometries. It is, however, possible that the absence of spin-dependent terms could produce an orbital degeneracy that is different than otherwise "exact" calculation. In that case, the computed structure can undergo larger than expected Jahn−Teller distortion. This effect will only be present in limited cases and may not play a significant role in understanding properties such as energetics and equilibrium geometries, discussed here. Indeed, ab initio density functional calculations show that the geometries of Ni clusters undergo minimal distortion with change in the spin-states.[40]

A direct way of assessing the validity of the potential in eq 2.1 is to compute the structures of small Ni clusters and compare these with first-principles calculations that take into account electron spin explicitly. This is done in Table 1 for Ni_n clusters up to $n = 6$ for which ab initio results[15] exist. Note that the agreement is, indeed, very good. We have also calculated the ground state magnetic moment and vertical ionization potential from first principles using the geometries obtained from molecular dynamics simulation, and our results agree quantitatively with experiment as well as independent ab initio molecular orbital calculations.[15,41] In addition, we have computed the energy difference between the isomers using many-body potential and first-principle calculations, and our results show a close agreement between the two.[41]

TABLE 1: Ground State Geometries, Bond Lengths, and Binding Energies for Ni_n ($n < 6$) Clusters (Values in Parentheses Correspond to ab Initio Results[15])

size	average bond length (Å)	binding energy (eV)
$n = 2$	2.01(1.99)	2.10(1.61)
$n = 3$	2.15(2.15)	2.50(1.96)
$n = 4$	2.20(2.17)	2.77(3.34)
$n = 5$	2.36(2.25)	2.90(2.83)
$n = 6$	2.43(2.33)	3.03(3.27)

III. Results and Discussions

We have studied the evolution of equilibrium geometries, average interatomic distances, coordination number, relative stability, and dominant fragmentation channels of Ni_n clusters for $2 \leq n \leq 23$. The studies enable us to identify the basic building block as the clusters grow and how the evolution in the geometry may be correlated with the underlying bonding mechanism. We discuss these results individually in the following.

A. Equilibrium Geometries. Determination of equilibrium geometries of clusters plays a central role in our understanding of the evolution of lattice structure as clusters grow. The equilibrium geometries are intimately related to the underlying electronic structure, and the preferred structure is the one for which the total energy reaches the minimum. It should be emphasized that the total energy depends on the electron distribution, which in turn depends on the atomic structure. While a quantitative evaluation of this self-consistent interaction is difficult, qualitative conclusions can still be drawn on equilibrium geometries once the dominant mechanism for the electron bonding is established. For example, in rare-gas systems the closed-shell configurations of atoms make the interatomic interaction weak. The equilibrium structures are then determined by maximizing the number of pairwise bonds and the structures assume close-packed geometries. This is also true for small clusters ($n < 10$) of Mg and other alkaline earth elements that have closed atomic shell (ns^2) configurations. However, as clusters grow, the hybridization between s- and p-states increases and the electrons assume a "metallic" character. The clusters then no longer resemble the geometries of rare-gas clusters. For clusters of simple-metal elements such as alkali metals, the electrons are nearly free and increased degeneracies allow the geometries to undergo Jahn−Teller distortions. In covalently bonded systems such as Si, the evolution of the geometries reveals that adding an atom does not significantly perturb the structure of the parent cluster. In Ni clusters, the bonding has contributions from the localized d-electrons as well as quasi-free sp-electrons. For large clusters, it is logical to assume that the electrons would exhibit strong metallic character. Correspondingly the equilibrium geometries would depart from the close-packed structures prevalent in rare-gas systems. It would be easy to distort the geometry of a preceding cluster by adding an atom. In very small clusters of transition metal atoms, the bonding may still be characterized by the localized nature of electrons and the corresponding atomic structures may be close-packed. For a lack of a better description, we will characterize the electrons in small clusters where the geometries are close-packed to be covalent-like. In large clusters where distortions in geometries are easy to induce, the electrons can be assumed to be metallic-like. A study of the evolution of geometries can, therefore, shed light on the

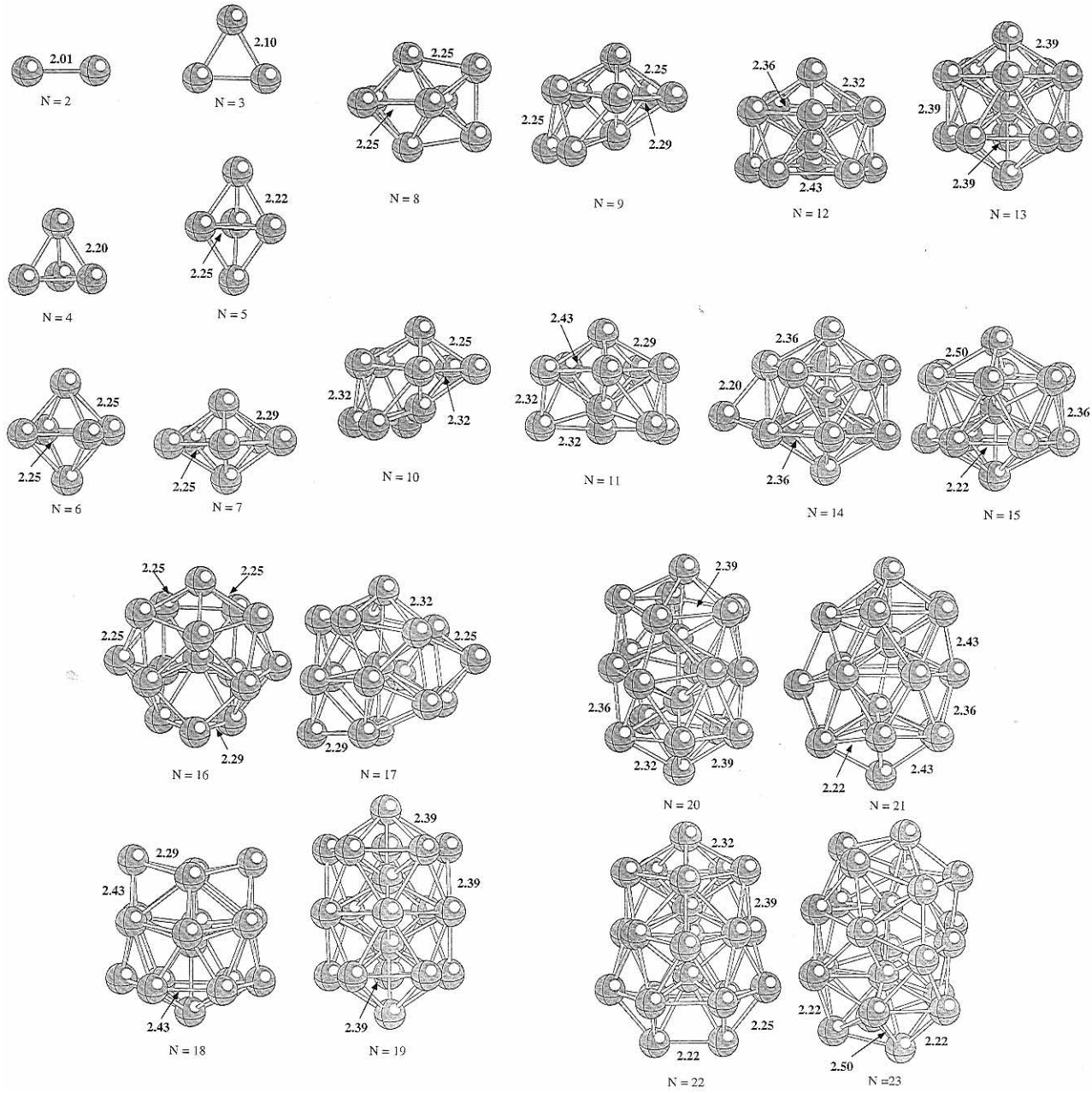

Figure 2. Equilibrium geometries of Ni_n ($2 \leq n \leq 23$) clusters.

underlying changes in the electronic structure as clusters grow. We also note that the average interatomic distance of semiconductor clusters decreases monotonically with increasing size, while the reverse is true for metallic clusters.

We define the average interatomic distance in a cluster as

$$\langle R \rangle = \frac{1}{N_b} \sum_{i,j} R_{ij} \tag{3.1}$$

where R_{ij} is the bond distance between two nearest neighbor atoms and N_b equals the number of such bonds. The average coordination number in a cluster is defined as

$$\mathrm{CN} = \frac{1}{N} \sum_{i} i N_i \tag{3.2}$$

where i is the number of atoms that have N_i number of nearest neighbor atoms in the cluster. N is the total number of atoms in the cluster. Unlike in the computation of $\langle R \rangle$, we consider any atom to be a nearest neighbor atom if it lies within a distance not exceeding 12% of the smallest bond distance. The factor 12% originates from the observation that two of the largest bonds in the Ni_{23} cluster differ by 12%.

We begin by making some general remarks on the equilibrium geometries shown in Figure 2. The physics behind each of the preferred geometries and the existence of isomers are discussed later in this section. In general, the geometries of clusters do not mimic the arrangements found in the bulk. Although the structures containing up to six atoms represent closely those found in rare-gas clusters, they differ sharply from the rare-gas structures at larger sizes. This departure is clearly due to the square root term in eq 2.1. Clusters containing seven and more atoms exhibit structures consisting of a pentagonal ring that is the backbone of an icosahedron. The structure of Ni_{13} is icosahedric. The average interatomic distance continues to rise monotonically (see Figure 3) with size until $N = 9$ but exhibits small oscillations for larger sizes, in contrast to what one observes in alkali metal clusters. Furthermore, the average bond distance of Ni_{23} is 2.25 Å and is about 10% shorter than the

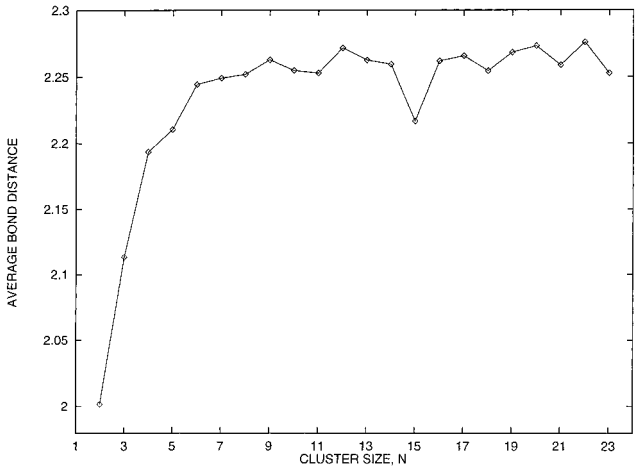

Figure 3. Plot of the average interatomic distance, $\langle R \rangle$, as a function of cluster size.

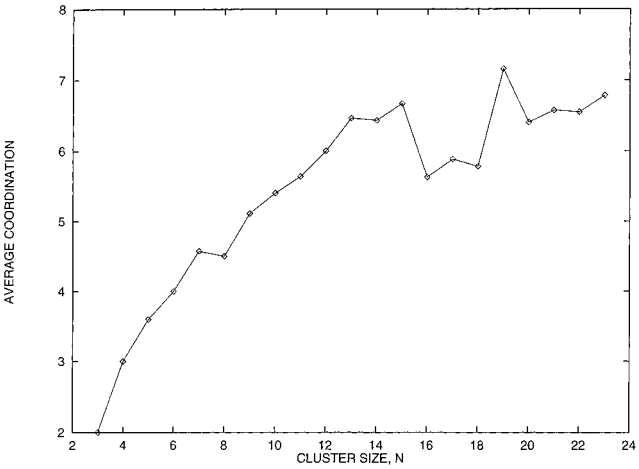

Figure 4. Plot of the average coordination number, CN, as a function of cluster size.

nearest neighbor distance in bulk Ni. These observations are in close agreement with a recent EXAFS experiment where Apai *et al.*[42] have measured the Ni−Ni distance at the lowest coverage (corresponding to a cluster diameter of 8 Å) to be 2.24 ± 0.04 Å. The coordination number in Figure 4 shows no sign of convergence to the bulk value (which is 12) and exhibits sharp variations with size. This is understandable since even for Ni_{23} there are 20 surface atoms and only three bulk atoms and the coordination number of surface atoms never exceeds 9. The role of coordination number on reactivity will be discussed later.

We now discuss the physics behind the individual geometries of clusters in four separate groups.

Ni_2−Ni_6. The equilibrium geometries of Ni_n clusters in this size range are very similar to those found in rare-gas clusters as well as metal clusters with closed atomic shells such as Mg_n clusters and are consistent with hard sphere packing. Note that the Ni_2 dimer bond length is 2.01 Å. This bond length is consistent with earlier theoretical studies. The experimental bond length lies between 2.15 and 2.2 Å. Our value is slightly smaller than the experimental bond length. For Ni_3 and Ni_4 we obtain a triangular and tetrahedral structure with interatomic distances of 2.1 and 2.2 Å, respectively. The ab initio calculation finds a distorted triangle for Ni_3 (with bond lengths of 2.18 and 2.15 Å) and a D_{2d} structure (with bond lengths of 2.11 and 2.74 Å) for Ni_4. In the case of Ni_5, our calculations lead to a triangular bipyramid with bond lengths of 2.25 and 2.22 Å compared to the corresponding ab initio bond lengths of 2.29 and 2.23 Å, respectively. The comparison shows that the many-body potential leads to geometries that are in reasonable agreement with ab initio results. Note that our many-body potential does not permit the Jahn−Teller distortions in small clusters obtained in the ab initio calculation that includes spin. The Ni_6 cluster is a perfect octahedron with a bond length of 2.25 Å. The atoms in each of these clusters are identical, and one does not expect any preferential sites for the chemical reaction. Examination of the structures of Ni_2−Ni_6 also illustrates how the geometries evolve as successive atoms are added. It appears that there is minimal rearrangement of the parent cluster as an atom is added to it; that is, the energy cost to rearrange the atomic configurations of the parent cluster must be large and is therefore avoided. This is the signature of "covalent bonding" among the atoms, as a covalent bond is more directional than a metallic bond. In free electron metal clusters, the delocalized nature of the electrons permits structural rearrangement.

To understand what factors govern the equilibrium geometries, we describe in Figure 5 some of the possible shapes clusters can take as a function of size. For $n = 3$, the structures can be either linear chain or triangular. The number of metal−metal bonds for the triangular structure is higher than that in the linear structure, and the former is found to correspond to the equilibrium geometry. For $n = 4$, the number of metal−metal bonds in the rhombus structure is 4, while it is 6 in the tetrahedral structure. As seen in Figure 2 the tetrahedral Ni_4 is the preferred structure. For $n = 5$ the structures in Figure 5e-g have respectively nine, eight, and five metal−metal bonds, and Figure 5e has the lowest energy. For $n = 6$, both structures in Figure 5h (octahedron) and Figure 5j (bicapped triangular bipyramid) have 12 metal−metal bonds, but the average coordination number for the structure in Figure 5h is 4, while that for Figure 5j is 3.6. Total energy minimization yields Ni_6 to have an octahedral preferred structure. Thus for clusters that have an equal number of metal−metal bonds, a secondary rule is that the structure that maximizes the coordination number has the lowest energy.

Ni_7. The Ni_7 cluster is a special case since a number of earlier theoretical calculations have predicted the preferred structure to be a pentagonal bipyramid, which is also the structure we calculate (see Figure 3). However, the experimental work on N_2 uptake was shown to be consistent with only the capped octahedron structure. This raises several interesting questions: (1) Is the capped octahedron structure another isomer of Ni_7? (2) If so, is it energetically degenerate with the pentagonal bipyramid structure? (3) Why does theory predict a structure that is inconsistent with the experimentally inferred structure? (4) The icosahedric structure of metal clusters requires the existence of a 5-fold ring. Although this could have occurred for Ni_5, it did not appear until Ni_7. All the structures until Ni_6 can be viewed as adding an atom to the previous cluster without modifying its original structure. This will also hold true for Ni_7 if the preferred structure is indeed a capped octahedron. However, for the Ni_7 to be a pentagonal bipyramid, major reconstruction of the octahedral Ni_6 structure is necessary as an atom is added. Alternatively, the existence of Ni_7 in the pentagonal bipyramid structure could point to the existence of an alternate channel for cluster growth with the pentagonal ring as a seed. Quantitative understanding of this possibility can only be achieved by a detailed simulation of the clustering process. Before we discuss this, we can provide a qualitative understanding of the preferred structure by examining the number of metal−metal bonds and coordination number of the two structures shown in Figure 5k,l. Both the structures have 15 metal−metal bonds. However, in the pentagonal bipyramid

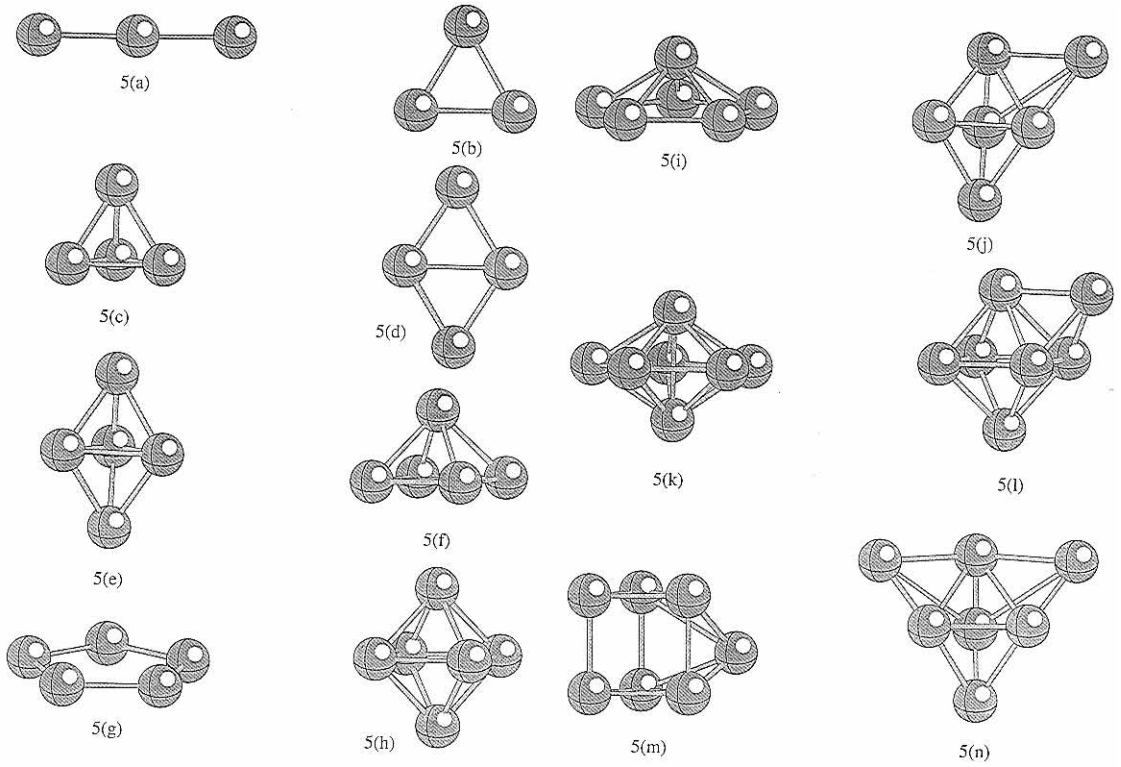

Figure 5. Possible structures a cluster can take as a function of cluster size.

structure there are two atoms with 6-fold coordination and five atoms with 4-fold coordination, yielding an average coordination number of 4.6. For the capped octahedron, there are three 5-fold coordinated, three 4-fold coordinated, and one 3-fold coordinated atom, yielding an average coordination number of 4.3. Thus, the structures in Figure 5k,l should be nearly degenerate. Indeed, our calculation shows that the total energy of the pentagonal bipyramid is 0.1 eV lower than the capped octahedron. The structure in Figure 5n also has 15 metal−metal bonds, but its average coordination number is even lower (4.1) than that in Figure 5l and is energetically unfavorable. We would like to add that the effective medium potential used by Stave and Depristo does not lead to the capped octahedron as one of the structures close in energy to the pentagonal bipyramid. The experimental data of Parks *et al.*[17] clearly point to the existence of a capped octahedron structure.

We discuss the coexistence of Ni_7 isomers vis à vis experimental observation in the latter part of this section.

Ni_8−Ni_{13}. The structure of Ni_8 is found to be bicapped octahedral and not capped pentagonal bipyramid, as seen in rare-gas clusters. Note that the bicapped octahedron has 19 metal−metal bonds, while the capped pentagonal bipyramid can only have 18 bonds. This further confirms the rule discussed above in favoring the former structure as the ground state. The growth sequence of Ni_9−Ni_{13} is toward the icosahedron structure. Ni_9 has a bicapped pentagonal structure, while the most stable structures for Ni_{10}−Ni_{12} are found by successively capping the triangular faces of the pentagonal bipyramid. Ni_{12} is found to be the icosahedron minus one atom. The ground state structure for Ni_{13} is an icosahedron.

Ni_{14}−Ni_{23}. The structure of the Ni_{14} cluster emerges by adding an atom to one of the pentagonal planes of the Ni_{13} cluster. This is in contrast to the rare-gas clusters, where the 14-atom cluster is a capped icosahedron. Thus the transition metal clusters can gain additional stability by modifying even the highly stable parent clusters. Ni_{15} is found to have a hexagonal antiprism structure with three atoms along the symmetric axis, again in sharp contrast to rare-gas clusters. The structures of Ni_{16} and Ni_{17} can only be constructed after significant modifications of the Ni_{15} and Ni_{16} structures, respectively. Symmetry returns as Ni_{18} forms and Ni_{19} assumes the structure of a double icosahedron. Ni_{20} has a D_{3d} symmetry structure as the most stable one. Ni_{21} has a structure with two hexagonal planes and one pentagonal plane with four atoms on the symmetric axis. Ni_{22} has a structure with three hexagonal planes. The global minimum configuration for Ni_{23} is found to be a polyicosahedral (three interpenetrating double icosahedra) cluster.

B. Comparison with Experiment. As mentioned earlier, there are no experimental techniques that can directly probe the geometry of small transition metal clusters. Attempts have been made to achieve structural information indirectly by chemical methods. For Ni clusters extensive studies of N_2 uptake as a function of temperature and pressure have been used to predict geometries for $4 < n < 29$ atom clusters.[17] This is done by examining the plateaus in the N_2 uptake and making the following assumptions. (1) N_2 binds to clusters in molecular form. (2) Binding of N_2 does not significantly alter the geometry of the metal cluster. (3) Ni atoms with four or fewer nearest neighbor metal atoms can bind two N_2 molecules at saturation. (4) Ni atoms with metal coordination number between 5 and 8 can bind one N_2 at saturation. (5) Ni atom with 9 metal−metal coordination can only weakly bind an N_2, and finally (6) Ni with more than nine nearest neighbor metal atoms cannot bind an N_2 molecule.

Assumption 1 is probably valid since it is known that N_2 binds molecularly on metal surfaces.[43] Furthermore, the binding energy of a N_2 molecule is 9.7 eV, while that of a NiN dimer is only 3.2 eV. Thus, it will be energetically unfavorable for N_2 to dissociate and bind to Ni in atomic form. This also holds for the binding of NO and CO to the Ni atom, but it is not true for H_2 interacting with Ni. Assumption 2 is likely valid for the same reason as discussed above: N_2 is an inert gas and interacts weakly with a metal cluster. The validity of assump-

TABLE 2: Metal−Metal Coordination as a Function of Cluster Size and the Comparison between N_2 Uptake Data Derived from Experiment (Ref 13) and That Computed from Structures Shown in Figure 2

cluster size	no. equivalent sites (coordination) $i(N_i)$; see eq 3.2	no. of N_2's bound: derived from structures in Figure 2	no. of N_2's bound: experimental plateaus
3	3(2)	6	8
4	4(3)	8	4, 8
5	2(3), 3(4)	10	5, 8
6	6(4)	12	6
7	5(4), 2(6)	12	1, 7, 8
8	4(4), 4(5)	12	7, 9
9	4(4), 2(5), 2(6), 1(8)	13	8
10	3(4), 3(5), 3(6), 1(9)	13	9
11	2(4), 4(5), 4(6), 1(10)	12	10
12	5 (5), 6(6), 1(11)	11	11
13	12(6), 1(12)	12	12
14	1(3), 9(6), 3(7), 1(12)	14	14
15	12(6), 2(7), 1(14)	14	12, 16
16	1(4), 7(5), 7(6), 1(9)	16	14, 16
17	2(4), 3(5), 11(6), 1(11)	16	16
18	2(4), 8(5), 8(7)	20	16, 17
19	12(6), 5(8), 2(12)	17	17
20	2(5), 16(6), 2(11)	18	17
21	1(4), 4(5), 8(6), 4(7), 2(8), 1(10), 1(12)	18	18
22	5(5), 9(6), 4(7), 2(8), 1(9), 1(12)	20	17
23	2(5), 12(6), 6(7), 1(8), 2(12)	21	18

tions 3−6 are difficult to assess, as there is no fundamental justification for it. More importantly, it is not at all clear whether these rules should apply to all clusters irrespective of their size. One knows that the electronic structure of clusters depends sensitively on their size.

To critically examine how well the above assumptions 3−6 are valid, we have calculated the number of N_2's a cluster can absorb at saturation by using these rules and the structures in Figure 2. We provide the details of the calculation in Table 2. The second column lists the number of equivalent atoms in each cluster, with their coordination number given in parentheses. For example, $i(N_i)$ means i number of atoms have N_i-fold metal−metal coordination. With the use of assumptions 3−6, the third column lists the maximum number of N_2's that can be bound to each of the clusters in Figure 2. The last column is taken from the plateaus of the N_2 uptake data and indicates the number of inequivalent sites in a cluster and the number of N_2's that can bind to these sites.

We note that the geometries of clusters containing 4, 12, 13, 14, 16, 17,19, and 21 atoms are consistent with the experiments. For Ni_5 and Ni_6 clusters Riley and co-workers[17] predicted the structures to be triangular bipyramid and regular octahedron, respectively, which is exactly what we calculate. However, the maximum N_2 uptake according to the above rules is clearly inconsistent with these geometries. This suggests the need to understand N_2 absorption on clusters on a more fundamental level. For example, ab initio calculations should be carried out to study the nature of N_2 interaction with metal clusters. Is N_2 bound molecularly? How many N_2's can be bound to a single Ni atom, and how does this number change as cluster size increases? Such calculations are presently underway and will be discussed in due course.

We now focus on the N_2 uptake on the Ni_7 cluster, which shows very interesting features. Riley and co-workers[17] have observed plateaus in the N_2 uptake at 1, 7, and 8; that is, Ni_7 readily binds one N_2 molecule and as conditions are altered it can bind seven and finally eight N_2 molecules. This is clearly inconsistent with a pentagonal bipyramid structure, which has two inequivalent sites (five 4-fold coordinated and two 6-fold coordinated atoms). The capped octahedron structure with a lone atom capping a triangular face will satisfy the experimental observation. No theoretical calculation studied so far has predicted this structure to be the ground state. As mentioned earlier, this cluster is found to be only 0.1 eV above the pentagonal bipyramid structure, and within the accuracy of our calculation, these two structures are degenerate. Thus, our calculation of Ni_7 structure provides a geometry that is indeed consistent with the experiment. We should emphasize that the existence of Ni_7 in the pentagonal bipyramid structure cannot be ruled out in the experiment, as Ni_7 in this structure can easily take seven N_2's and there is a plateau at 7 in the experimental data. Further experiments may be necessary to distinguish between the two isomers, and we address this in detail in a separate paper.[41]

Riley and co-workers also find no strong evidence for pentagonal growth for Ni_{10}−Ni_{12}. This is contrary to what we see in Figure 2, where the pentagonal growth is clearly visible. We consider Ni_{11} in particular. If we disregard the only Ni atom that has 10 metal−metal coordination, the remaining 10 atoms of Ni_{11} could bind 10 N_2's, which is exactly the plateau Riley and co-workers observe. We fail to see a plateau at either 13 or 14, as described by these authors.

To conclude this section, it is fair to say that the structures derived here can indeed be consistent with the experimental N_2 uptake data if the assumptions of how many N_2's can bind to a particular site are not fixed for all clusters. Therefore, there is a need to understand the nature of N_2 binding to clusters at a fundamental level.

C. Stability, Energetics, and Reaction Channels. The relative stabilities of the clusters described in the above can be studied by analyzing their energetics. We consider here the evolution of the binding energy, E_b, the difference in energy in adding an atom to the preceding cluster, ΔE, and the second-order derivative, $\Delta' E$ of the total energy. These energies are defined as

$$E_b(n) = -[E(n) - nE_0]/n \tag{3.3}$$

$$\Delta E(n) = E(n) - E(n-1) \tag{3.4}$$

$$\Delta' E(n) = E(n+1) - E(n-1) - 2E(n) \tag{3.5}$$

In the limit of very large clusters both E_b and ΔE will approach the cohesive energy of the corresponding bulk solid. The extent to which E_b and ΔE differ is a signature of how different the clusters are from their bulk limit in terms of stability.

It has been demonstrated for alkali metal clusters that ΔE and $\Delta' E$ show odd−even alternation with pronounced features at $N = 2, 8, 20, 40, ...$[44] These are referred to as magic numbers and correspond to the most stable clusters. Since the electrons in a transition metal cluster are not free-electron-like, one would not expect the energetics of Ni_n clusters to mimic the structures seen in alkali metal clusters.

In Figure 6 we plot the binding energy as a function of cluster size. The binding energy evolves monotonically, but the binding energy per atom of the largest cluster (3.5 eV) is still much lower than the cohesive energy of the solid, which is 4.44 eV.

The energy difference, ΔE, in adding an atom to the preceding cluster is plotted in Figure 7. It does show odd−even alternation up to the Ni_7 cluster, but this trend disappears for larger clusters. Secondly, there are no pronounced structures except those of Ni_2 and Ni_{13} that can be identified as magic numbers. This can be seen more clearly in the second derivative of the total energy, $\Delta' E$ plotted in Figure 8 where for $n = 2$ and 13 there

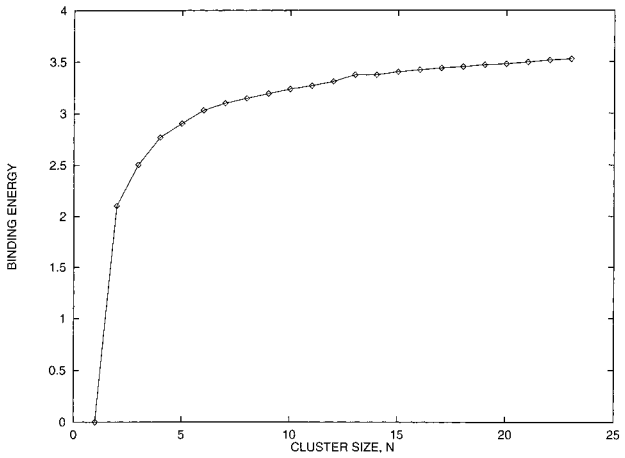

Figure 6. Plot of binding energy per atom, $E_b(n)$, as a function of cluster size.

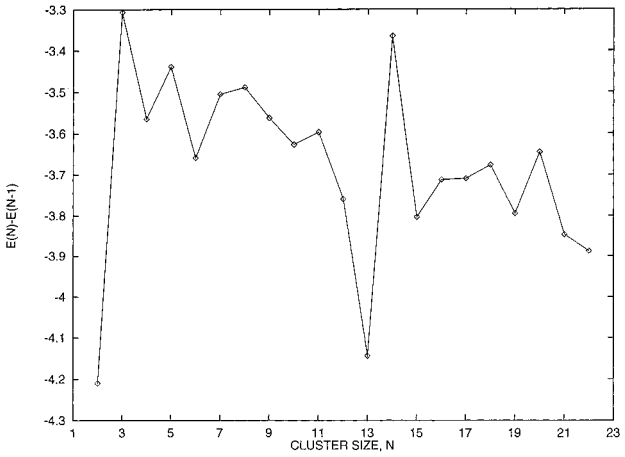

Figure 7. Plot of "cohesive energy", $\Delta E(n)$, as a function of cluster size. For details see the text.

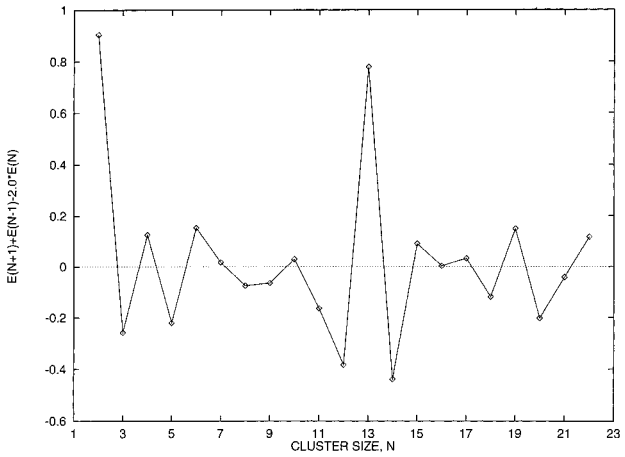

Figure 8. Plot of second energy difference of the total energy, $\Delta' E(n)$ (see the text for definition), as a function of cluster size.

are pronounced peaks. Results in Figures 6−8 clearly indicate that there is no similarity between the electronic structure of Ni_n and alkali metal clusters, just as there is no resemblance between the geometries of these two classes of clusters. Even in small clusters, the electronic structure of transition metal clusters shows unique features not seen in simple-metal clusters.

This can be further demonstrated by studying the fragmentation energies as a cluster of n-atoms fragment to m and $(n - m)$ clusters. In the case of alkali metal clusters it was predicted that in neutral clusters[45] those consisting of magic number atoms (2, 8, 20, ...) will be the predominant fragmentation products.

TABLE 3: Lowest and Next Highest Fragmentation Energy for Ni Clusters

cluster size (N)	fragmentation channels ($N = m + n$)	dissociation energy (eV)
4	2, 2	2.66
	3, 1	3.56
5	3, 2	2.79
	4, 1	3.44
6	4, 2	2.88
	3, 3	3.15
7	5, 2	2.95
	4, 3	3.08
8	6, 2	2.78
	4, 4	3.01
9	7, 2	2.84
	6, 3	3.04
10	8, 2	2.98
	6, 4	3.10
11	9, 2	3.01
	7, 4	3.19
12	10, 2	3.15
	6, 6	3.36
13	11, 2	3.69
	8, 3	3.90
14	12, 2	3.30
	13, 1	3.37
15	13, 2	2.95
	12, 3	3.80
16	14, 2	3.30
	13, 3	3.36
17	15, 2	3.20
	13, 4	3.50
18	16, 2	3.17
	15, 3	3.58
19	17, 2	3.26
	16, 3	3.66
20	18, 2	3.23
	19, 1 (17, 3)	3.60
21	19, 2	3.28
	18, 3	3.70
22	20, 2	3.50
	21, 1 (19, 3)	3.80
23	21, 2	3.45
	22, 1	3.70

If the parent cluster is singly positively charged, the preferred channels will shift to $n = 3, 9, ...$[45] This prediction has since been verified.[46] Since in the transition metal clusters there are no magic numbers, the preferred channels can be investigated by calculating the dissociation energy,

$$\Delta D(m) = E(n) + E(m) - E(n + m) \qquad (3.6)$$

where $E(n)$, $E(m)$, and $E(n + m)$ are the total energies of clusters of n, m, and $(n + m)$ atoms, respectively. Table 3 contains the channels corresponding to lowest and next highest energy, ΔD for Ni clusters. It can be noted here that the dimer is found to be the most favorable channel for Ni_n in the size range $n \leq 24$. (This is consistent with Figure 8, where Ni_2 is found to exhibit unusual stability.) For clusters larger than $n = 13$, other channels also have very close fragmentation energy. We would like to caution the reader that the above analysis for dissociation channels is based on the total energy difference only. In actual fragmentation, the energy barriers can play an important role. We will discuss this aspect along with the temperature-dependent dynamics of Ni clusters in a forthcoming paper and compare with experiments involving collision-induced fragmentation.

IV. Conclusions

In summary, we have calculated the equilibrium geometries, relative stabilities, and dominant fragmentation channels of Ni_n

($n \leq 23$) clusters using an efficient molecular dynamics simulation technique and a semiempirical many-body interatomic potential. The equilibrium geometries are governed by maximizing the number of metal−metal bonds. The geometries are found to be very different from either the rare-gas or simple-metal clusters and cannot be characterized as fragments of the fcc structure. While for very small clusters ($n \leq 7$) the evolution of geometry can be viewed as adding an atom to the preceding cluster without significantly modifying its structure, distortions in the cluster structure is seen in larger clusters. The icosahedral growth pattern is observed starting from the Ni_9 cluster. However, for clusters such as Ni_{14} and Ni_{15}, the atoms do not simply cap the icosahedric structure of Ni_{13}, but rather start forming a hexagonal ring structure. Most of the structures are consistent with those derived from the N_2 uptake data if one assumes that a metal atom with more than 9 metal−metal coordination cannot bind a N_2 molecule while every other exposed Ni atom can bind one N_2 molecule. The existence of cluster isomers has also been identified. In particular, Ni_7 has been found to exist in two nearly degenerate forms: a capped octahedron and a pentagonal bipyramid.

The average interatomic distance evolves monotonically toward the bulk limit even though for the Ni_{23} cluster it is still 10% less than the bulk value. The average coordination number, on the other hand, varies strongly with cluster size and shows no sign of convergence to the bulk value of 12. We also find no correlation between the average coordination number and the plateaus in the N_2 uptake data.

The binding energy per atom in the cluster evolves monotonically with size, while the energy difference in adding an atom to the preceding cluster and the second-order derivative of the total energy show sharp oscillations. The convergence of the binding energy per atom to the bulk cohesive energy is slow, and there are no magic numbers, as found in alkali metal clusters. Ni_2 and Ni_{13} clusters show enhanced stability compared to other clusters and form dominant products in the fragmentation of neutral Ni clusters.

Acknowledgment. This work is supported in part by a grant from the Department of Energy (DE-FG05-87ER45316). S.K.N. would like to thank Dr. J. Jellinek for many useful discussions.

References and Notes

(1) Berry, R. S.; Burdett, J.; Castlemann, A. W., Jr. *Z. Phys*. **1993**, 23.
(2) Jena, P.; Khanna, S. N.; Rao, B. K. *Physics and Chemistry of Finite Systems: From Clusters to Crystals*; Kluwer Dordrecht, 1992.
(3) Jellinek, J.; Guvenc, Z. B. In *The Synergy Between Dynamics and Reactivity at Clusters and Surfaces*; Farrugia, L. J., Ed; Kluwer: Dordrecht, 1995; p 159.
(4) Khanna, S. N.; Jena P. *Phys. Rev. Lett.* **1992**, *69*, 1664; *Phys. Rev. Lett.* **1993**, *71*, 208.
(5) Harris, J.; Jones, R. O. *J. Chem. Phys.* **1979**, *70*, 830.
(6) Basch, H.; Newton, M. D.; Moskowitz, J. *J. Chem. Phys.* **1980**, *73*, 4492.
(7) Tomonari, M.; Tatewaki, H.; Nakamura, T. *J. Chem. Phys.* **1986**, *85*, 2875.
(8) Bonacic-Koutecky, V.; Fantucci, P.; Koutecky, J. *Chem. Rev.* **1991**, *91*, 1035.
(9) Mlynarski, P.; Salahub D. R. *J. Chem. Phys.* **1991**, *95*, 6050.
(10) Nygren, M. A.; Sigbahn, P. E. M.; Wahlgren, U.; Akeby, H. *J. Chem. Phys.* **1992**, *96*, 3633.
(11) Rosch, N.; Ackermann, L.; Pacchioni, G. *Chem. Phys. Lett.* **1992**, *199*, 275. Rao, B. K.; Jena, P.; Ray, A. K. *Phys. Rev. Lett.* **1996**, *76*, 2878.
(12) Pou-Amerigo, R.; Merchan, M.; Nebot-Gil, I.; Malmqvist, P. A.; Boss, B. O. *J. Chem. Phys.* **1994**, *101*, 4893.
(13) Castro, M.; Salahub, D. R. *Phys. Rev. B* **1993**, *47*, 10955.
(14) Ballone, P.; Jones, R. O. *Chem. Phys. Lett.* **1995**, *233*, 632.
(15) Reuse F. A.; Khanna S. N. *Chem. Phys. Lett.* **1995**, *234*, 77.
(16) Sarkas, H. W.; Arnold, S. T.; Handricks, J. H.; Bowen, K. H. *J. Chem. Phys.* **1995**, *102*, 2653. Schulze Icking-Konet, G.; Handschuh, H.; Gantefor G.; Eberhardt, W. *Phys. Rev. Lett.* **1996**, *76*, 1047.
(17) Parks, E. K.; Zhu, L.; Ho, J.; Riley, S. J. *J. Chem. Phys.* **1994**, *100*, 7206; *J. Chem. Phys.* **1995**, *102*, 7377. Parks, E. K.; Riley S. J. *Z. Phys. D* **1995**, *33*, 59.
(18) Jellinek, J.; Garzon, I. L. *Z. Phys. D* **1991**, *20*, 239. Garzon, I. L.; Jellinek, J. in ref 2, Vol. 1, p 405; *Z. Phys. D* **1991**, *20*, 235; *Z. Phys. D* **1993**, *26*, 316. Guvenc, Z. B.; Jellinek, J.; Voter, A. F. In ref 2, Vol. 1, p 411. Guvenc, Z. B.; Jellinek, J. *Z. Phys. D* **1993**, *26*, 304. Lopez, M. J.; Jellinek, J. *Phys. Rev. A* **1994**, *50*, 1445.
(19) Uppenbrink, J.; Wales, D. J. *J. Chem. Soc., Faraday Trans.* **1991**, *87*, 215; *J. Chem. Phys.* **1992**, *96*, 8520; *J. Chem. Phys.* **1993**, *98*, 5720.
(20) Cleveland, C. L.; Landmann, U. *J. Chem. Phys.* **1991**, *94*, 7376.
(21) Stave, M. S.; De Pristo, A. E. *J. Chem. Phys.* **1992**, *97*, 3386.
(22) Blaisten-Barojas, E.; Khanna, S. N. *Phys. Rev. Lett.* **1988**, *61*, 1477.
(23) Gupta, R. P. *Phys. Rev. B* **1981**, *23*, 6265.
(24) Finnis, M. W.; Sinclair, J. E. *Philos. Mag.* **1984**, *50*, 45.
(25) Sutton, A. P.; Godwin, P. D.; Horsfield A. P. *MRS Bull*. **1996**, *21*, 42.
(26) Kirkpatrick, S.; Gelatt, C. D., Jr.; Vecchi, M. P. *Science* **1983**, *220*, 671.
(27) Lian, L.; Su, C.-X.; Armentrout, P. B. *J. Chem. Phys.* **1992**, *96*, 7542.
(28) Car, R.; Parrinelo, M. *Phys. Rev. Lett.* **1985**, *55*, 2471.
(29) Sutton, A. P.; Chen, J. *Philos. Mag. Lett.* **1990**, *61*, 139.
(30) Todd, B. D.; Lynden-Bell, R. M. *Surf. Sci.* **1993**, *281*, 191.
(31) Frenken, J. W. M.; Smeenk, R. G.; Van der Veen, J. F. *Surf. Sci.* **1983**, *135*, 147.
(32) Adams, D. L.; Petersen, L. E.; Sorensen, C. S. *J. Phys. C* **1985**, *18*, 1753.
(33) Demuth, J. E.; Marcus, P. M.; Jespen, D. W. *Phys. Rev. B* **1975**, *11*, 1460.
(34) Ning, T.; Yu, Q.; Ye, Y. *Surf. Sci*. **1988**, *206*, L857.
(35) Allen, M. P.; Tildesly, D. J. *Computer Simulation of Liquids*, Oxford University Press: Oxford, 1987.
(36) Berry, R. S.; Jellinek, J.; Natanson, G. N. *Phys. Rev. A* **1982**, *25*, 978. Beck, T. L.; Jellinek, J.; Berry, R. S. *J. Chem. Phys.* **1987**, *87*, 545. Wales, D. *Mol. Phys.* **1993**, *28*, 151.
(37) Stillinger, F.; Weber, T. *Phys. Rev. A* **1982**, *25*, 978.
(38) Briant, C. L.; Burton, J. J. *Nature Phys. Sci.* **1973**, *243*, 100; *J. Chem. Phys.* **1975**, *63*, 2045.
(39) Nayak, S. K.; Jena, P.; Bhattacharya, A.; Mahanti, S. D. To be published.
(40) Reuse, F. A.; Khanna, S. N.; Bernel, S. *Phys. Rev. B* **1995**, *52*, R11 650.
(41) Nayak, S. K.; Reddy, B. V.; Rao, B. K.; Khanna, S. N.; Jena P. *Chem. Phys. Lett.* **1996**, *253*, 390. Reddy, B. V.; Nayak, S. K.; Khanna, S. N.; Rao, B. K.; Jena, P. To be published.
(42) Apai, G.; Hamilton, J. F.; Stohr, J.; Thompson, A. *Phys. Rev. Lett.* **1979**, *43*, 165.
(43) Rao, C. N. R.; Rao, G. R. *Surf. Sci. Rep.* **1991**, *13*, 229.
(44) Knight, W. D.; Clemenger, K.; de Heer, W. A.; Saunders, W. A.; Chou, M. Y.; Cohen, M. L. *Phys. Rev. Lett.* **1984**, *52*, 2141.
(45) Jena, P.; Rao, B. K.; Nieminen, R. *Solid State Commun.* **1986**, *59*, 509. Rao, B. K.; Jena, P.; Manninen, M.; Nieminen, R. M. *Phys. Rev. Lett.* **1987**, *58*, 1188.
(46) Brechinac, C.; Cahuzac, Ph.; Cartier, F.; de Frutos, M.; Barnett, R. N.; Landmann, U. *Phys. Rev. Lett.* **1994**, *72*, 1636.